Int. J. Electrochem. Sci., 10 **(2015)** 5479 - 5487

International Journal of
ELECTROCHEMICAL
SCIENCE
www.electrochemsci.org

Short Communication

Enhanced Charge-Transfer Performance of Photoelectrode Based on Interface Modification in Dye-Sensitized Solar Cells

Y. Yang, Y.H. Qiang[*]*, J. Song, Z. Xing, C.B. Song*

School of Materials Science and Engineering, China University of Mining and Technology, Xuzhou 221116, China
[*]E-mail: yhqiang@cumt.edu.cn

Received: 26 March 2015 / *Accepted:* 29 April 2015 / *Published:* 27 May 2015

A simple FTO conductive glass substrate decoration by graphene nanosheets before the manufacture of TiO_2 photoelectrode via a layer by layer assembly process was proposed in dye-sensitized solar cells (DSSCs). FESEM images indicated that graphene nanosheets overlaid on FTO glass clearly. The *J-V* measurements of DSSCs demonstrated that introduction of graphene nanosheets on photoelectrode certainly presented obvious influence on photovoltaic performance. Exactly, as the amount of graphene additions increasing, conversion efficiencies of DSSCs firstly improved from 5.01% to 5.36% and then reduced to 3.67%, compared to the efficiency of 4.72% with bare FTO glass. EIS results exhibited that the charge transfer resistance (R_3) at TiO_2-FTO glass interface decreased as the addition of graphene nanosheets. When the substrate was treated by graphene solution twice, R_3 of corresponded DSSC (G2) was only 9.31 Ω, which is remarkably lower than that of the untreated one (15.01 Ω). This result revealed the interface modification function of graphene between FTO and TiO_2 film. However, as the treatment times increased further, R_3 rose to 11.32 Ω. This trend could be attributed to the electrocatalytic activity of graphene for I_3^- reduction which would be enhanced as the thickness of graphene film increased. This paper expounded that graphene nanosheets surface treatment of photoelectrode was an effective way to improve their photovoltaic performance in DSSCs.

Keywords: Dye-sensitized solar cells, Graphene nanosheets, Photoelectrode, Interface modification

1. INTRODUCTION

Dye-sensitized solar cells (DSSCs) have attracted considerable attention all over the world as potential substitutes for silicon based solar cells due to their low costs, relatively high photoelectric conversion efficiency and simple fabrication process [1-3]. The DSSCs have a sandwich configuration that consists of a dye-sensitized photoelectrode, an electrolyte containing I^-/I_3^- redox couple, and a Pt-

coated counter electrode [4]. The photoelectrode plays a more important role in photovoltaic performance than all other components of DSSCs, and some characteristic properties of photoanode materials, including morphology, phase structure and crystalline size decide their specific performance [5, 6]. In general, photoelectrode is a kind of nanocystalline film consisted of wide bandgap seimconductor materials. It serves to load dyes, accept and transport electrons [7, 8]. TiO_2 is considered to be an excellent photoelectrode material as a result of its advantages of high chemical stability, low price and non-toxicity, etc [9-12]. Nevertheless, the electron transfer in TiO_2 nanocrystalline film is a fleetly dynamic process of electron transmission and electron-hole pairs recombination, which directly affect the performance of DSSCs [13]. Therefore, various advanced materials and optimized methods have been widely studied for photoelectrodes design to improve the electron transmission and reduce the charge recombination [14-16].

Recently, as a single-layer hexagonal lattice composed by sp2 hybridized carbon atoms and a novel two-dimensional (2D) structure material with a theoretical thickness of 0.34 nm, graphene shows great promising properties in opto-electronics [17-21]. It holds some outstanding and unique characteristics such as good optical transparency, high specific surface area and excellent electronic transport efficiency [22-25]. Particularly, Fang et al. prepared different graphene-P25 composites photoelectrodes via a ball milling method for DSSCs which exhibited considerable photovoltaic performance [26]. Kim et al. fabricated graphene-linked TiO_2 anode by adding graphite oxide into titanium tetraisopropoxide solution, and the produced DSSC showed superior solar energy conversion efficiency of approximately 6.05% [27]. More recently, Chen et al. found the enhanced photovoltaic performance of DSSC using graphene-TiO_2 photoelectrodes prepared by in situ simultaneous reduction-hydrolysis technique [28]. However, as we know, there are little reports on surface modification on FTO glass substrate using graphene materials in DSSCs. Graphene that exists between TiO_2 film and FTO layer may induce some interesting results as its particular optical and electrical performance.

Herein, we design a simple process to make graphene coated FTO glass substrate prior to photoelectrode fabrication, and the schematic diagram are shown in Scheme 1. When ultrathin graphene nanosheets are inserted, as a result of its special work function, the surface of FTO behaves an excellent property of collecting electron. Therefore, this special structure of photoelectrode is expected to reduce charge recombination at FTO/TiO_2 interface and accelerate electron-hole pairs separation [29-32].

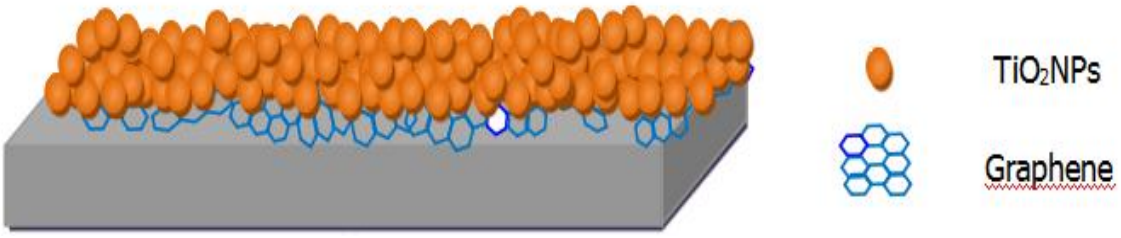

Scheme 1. Schematic illustration of the photoelectrode with graphene-treated substrate.

2. EXPERIMENTS AND CHARACTERIZATION

2.1 Preparation of graphene nanosheets

Graphene nanosheets (GNs) were synthesized by reduction of graphene oxide according to the modified Hummers method [33, 34]. Graphite, sodium nitrate ($NaNO_3$), and concentrated sulfuric acid (H_2SO_4) were mixed completely in a beaker by stirring at 0 °C ice-bath, and then potassium permanganate ($KMnO_4$) was added slowly to the mixed solution. The obtained mixture was removed to a 35 °C water-bath and stirred for 5 h. Subsequently, a certain amount of deionized water was added to the mixture and heated to 90 °C under stirring. After 20 minutes, the solution was diluted and followed by the addition of hydrogen peroxide (H_2O_2). Finally, the yellow-brown graphite oxide powder were gained by filtration and then washed with deionized water. To obtain graphene nanosheets, hydrazine hydrate was dropped slowly to graphite oxide solution under constantly stirring. And the graphene nanosheets powders were collected by centrifugation and dried at 60 °C overnight.

2.2 Fabrication of the graphene nanosheets pretreated photoelectrodes

The graphene nanosheets were dispersed in 2-propanol by ultrasonication for about 1h, and the dispersions (10^{-3} mg/ml) could be stable for a long time without marked sedimentation. This solution was spin-coated on FTO glass (15 Ω per square, Dalian Hepta Chroma), and a uniform semitransparent film was obtained after drying at room temperature. TiO_2 pastes were prepared by diluting commercial TiO_2 nanoparticles (size about 10 nm, Wuhan Geao) slurry with terpineol which could be easily made into film by spin-coating method on the graphene/FTO substrate without cracks. The films were dried at 60 °C for 15 min and then annealed at 450 °C for about 1 h. After sintering and cooling down to room temperature, the nanostructured films were immersed into the dye solution (0.3 mM N719, Dalian Hepta Chroma) in ethylalcohol for 24 h and the corresponding photoelectrodes were obtained. Four different photoelectrodes (denote as G0-G3) were prepared by varying spin-coating times of graphene nanosheets solution from zero to three.

2.3 DSSCs assembly and characterization

The sensitized GNs/TiO_2 photoelectrode and Pt-coated counter-electrode were sealed with 60 μm thick thermal-plastic surlyn (DHS-SN1760) spacer and assembled into a sandwich type cell. The electrolyte solution (0.6 M DMPII, 0.03 M I_2, 0.5 M TBP and 0.1 M LiI in MPN, Dalian Hepta Chroma) was injected into the device by capillary force using a fine 1 mL syringe.

The morphologies and microstructures of the coated graphene layers were characterized by field-emission scanning electron microscopy (FESEM, S-4800). The synthesized graphene nanosheets powders were examined by X-ray diffraction (XRD, D8 Advance). UV-visible transmittance spectra (UV-vis, Cary 300) of the graphene layers were obtained over the special range of 260 to 600 nm. The current density-voltage (*J-V*) characteristics of the assembled cells were measured under AM 1.5 simulated illumination (Beijing Trusttech) with a power density of 100 mW/cm^2 and a shining area of

0.25 cm^2 with a mask. Electrochemical impedance spectroscopy (EIS) analysis was made under illumination by using an electrochemical test station (CHI660D).

3. RESULTS AND DISCUSSION

3.1 Electrodes microstructure analysis

Fig.1 shows the XRD patterns of the prepared graphene nanosheets powders. The peak at 2θ = 26.7°could be attributed to diffraction of (002) lattice plane of graphite (JCPDS, 65-6212), indicating that the graphene oxide was reduced successfully.

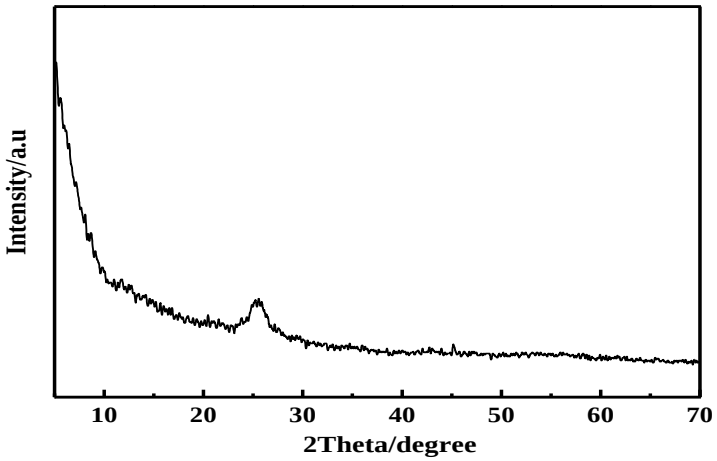

Figure 1. XRD pattern of the graphene nanosheets powders.

The FESEM images of graphene decorated FTO glass under different spin-coating times are shown in Fig. 2. It is clear that graphene particles with varied sizes scatter on FTO glass randomly, forming graphene nanosheets islands. As spin-coating times increase, the surface coverage of graphene nanosheets on FTO glass increases obviously and particles aggregation becomes serious at the same time.

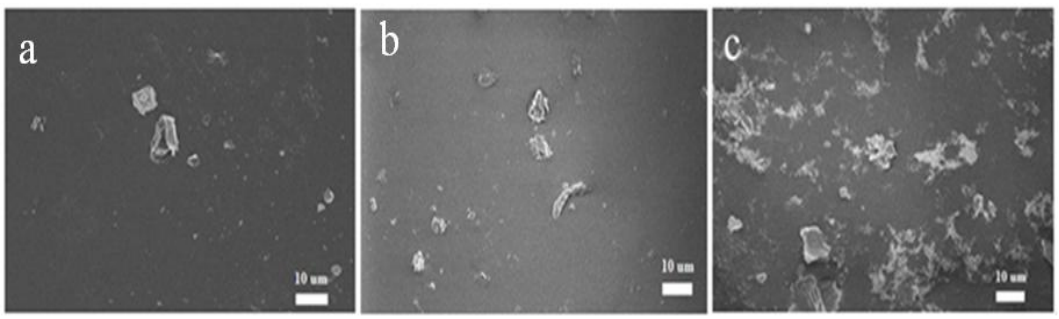

Figure 2. FESEM images of FTO surfaces pretreated by graphene of device G1(a), G2(b), and G3(c).

3.2 Optical performance of photoelectrode substrates

The UV-visible transmittance spectra of FTO conductive glass with and without graphene nanosheets treatments (G0, G1, G2, G3) are shown in Fig. 3. In the short wavelength region (<375 nm), both the original FTO substrate and the graphene-spin-coated substrates show the same behavior, the penetrated light decrease seriously. In the long wavelength region (>400 nm), the optical transmittance is only slightly reduced with increasing the amount of graphene additives as the light-scattering ability of graphene. This observation indicates the excellent optical transmittance of the spin-coated graphene nanosheets film.

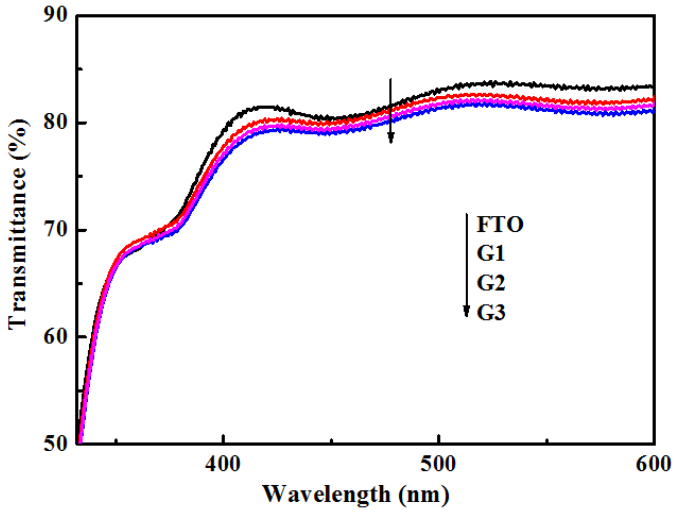

Figure 3. UV-vis spectra of graphene pretreated and bare FTO glass.

3.3 J-V characteristics

Fig. 4 displays the *J-V* characteristics parameters of the DSSCs based on pure TiO_2 photoelectrode and grpaphene pretreated photoelectrode. Meanwhile, the corresponding photovoltaic parameters are summarized in Table 1, including short-current density (J_{sc}), open-circuit voltage (V_{oc}), fill factor (FF) and photoelectric conversion efficiency (η). As seen, the η of G1 assembled DSSC (5.01%) is higher than pure TiO_2 DSSC (4.72%). This enhancement may be ascribed to the addition of graphene nanosheets, which greatly improve electron transfer efficiency from TiO_2 film to FTO substrate. When the spin-coating times of graphene nanosheets solutions increases to 2, the η of corresponding DSSC reaches an optimal value of 5.36%, and the J_{sc} of 15.79 $mA \cdot cm^{-2}$ is obtained. However, further increasing the spin-coating times, G3 assembled DSSC decreases sharply to 3.67% and 11.68 $mA \cdot cm^{-2}$ in η and J_{sc}, respectively. The results suggest that DSSCs efficiency is not in linear relation with the amount of graphene spin-coated on FTO glass substrate. Although graphene presents better electroconductivity than FTO, optical absorption of graphene layer would ascend as their thickness increase. Moreover, graphene exihibit some electrocatalytic performance for I_3^- reduction which would provide more electron recombination cites in photoelectrode [35-37]. By the way, the

grain boundaries existed among graphene particles is not benefit for electron transfer in graphene layer. Therefore, it is reasonable that G2 assembled DSSC presents the best photovoltaic performance. The detailed mechanism will further discusse based on electrochemical impedance spectroscopy measurements as following.

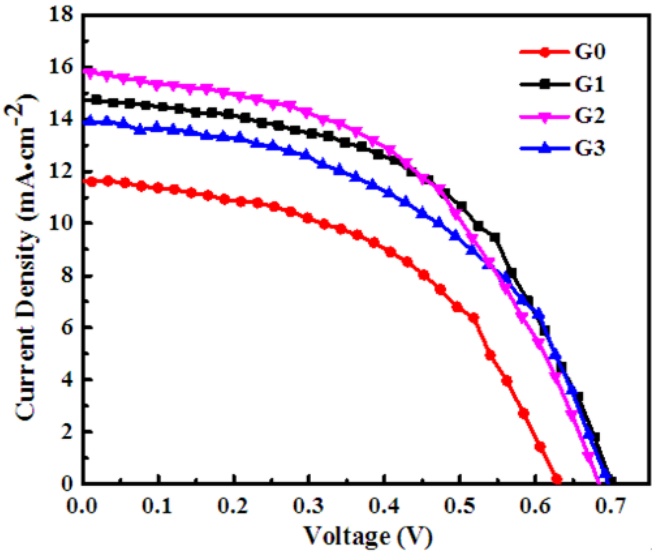

Figure 4. *J-V* curves of DSSCs with different photoelectrodes.

Table 1. Electron transfer resistance and photovoltaic parameters of the DSSCs operated under 1 Sun illumination.

Photoelectrode	R_3 (Ω)	J_{sc} (mA·cm^{-2})	V_{oc} (V)	FF	η (%)
G0	15.01	13.91	0.69	0.491	4.72
G1	9.78	14.73	0.69	0.493	5.01
G2	9.31	15.79	0.69	0.491	5.36
G3	11.32	11.68	0.63	0.499	3.67

3.4 EIS measurements

The EIS results of DSSCs with G0, G1, G2, and G3 photoelectrodes are presented in Fig. 5. The impedance spectrum shows two semicircles in the frequency range from 100 KHz to 10 mHz. The small and large semicircles in the high and low frequency ranges are related to the charge transfer processes at the Pt-coated counter electrode (R_2) and graphene/TiO_2/dye/electrolyte interface (R_3), respectively [38-40]. The Nyquist plots are simulated by an equivalent circuit containing constant phase element (CPE1 and CPE2), series resistance (R_1), and charge transfer resistance (R_2 and R_3) [34, 41]. Compared to the pure-TiO_2 DSSC (G0), the second semicircle decreased significantly due to the introduction of graphene layer. It is notable that the electron flow from the lowest unoccuoied molecular (LUMO) level of the dye to the FTO through the conduction band of graphene/TiO_2 became more effective [26]. Exactly, R_3 values (as shown in Table 1.) firstly decreases and then increases with rising the spin-coating times of graphene nanosheets. The lowest value is only 9.31 Ω in G2 assembled

DSSC which coincides with its highest power conversion efficiency in all the three DSSCs. For G3 assembled DSSC, its series resistance (R_1) is much lower than others as the good coverage of graphene on FTO glass, but its charge transfer resistance on graphene/TiO_2/dye/electrolyte interface (R_3) turns much higher than G1 and G2. As the large surface and electrocatalytic activity for I_3^- reduction of graphene, electron recombination on graphene/TiO_2/dye/electrolyte interface could become more serious with graphene coverage increase [35-37]. Therefore, photovoltaic performances of these four DSSCs are competition results of electron transfer acceleration and electron recombination enhancement effects of graphene layer. In other words, when graphene layer is thin, its electron transfer acceleration effect plays primary position, conversely, the electron recombination dominates while the graphene thickness is thick.

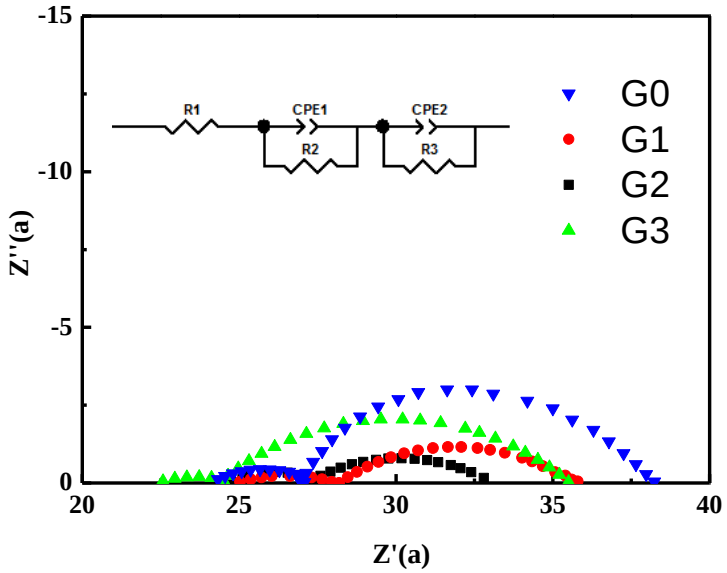

Figure 5. Nyquist plots of the DSSCs based on the different photoelectrodes. The top inset indicates the equivalent circuit.

4. CONCLUSIONS

In conclusion, we synthesized graphene nanosheets by hydrazine reduction of exfoliated graphite oxide. Furthermore, a simple and available method was demonstrated to enhance the power conversion efficiency by modifying the surface of FTO substrate with graphene nanosheets. The results showed that the photovoltaic performance first increased and then decreased with ascending amount of graphene additives. Importantly, spin-coating twice of graphene nanosheets onto the FTO substrate, the optimized DSSC was obtained and the final J_{sc} and η were increasing obviously by 13.52% and 13.56%, respectively. The enhancement was mainly due to improving electron transfer efficiency from TiO_2 film to FTO through graphene layer. However, electron recombination could become severe when excess graphene nanosheets existed. This method of pretreating FTO substrate with graphene nanosheets provides alternative approach to improve properties of DSSCs.

ACKNOWLEDGEMENTS
This work was financially supported by the Fundamental Research Funds for the Central Universities (2013XK07) and partial supported by Natural Science Foundation of Jiangsu Province (BK20130198).

References

1. M. Grätzel, B. O'Gegan, *Nature* 355 (1991) 737.
2. M. Grätzel, *Acc. Chem. Res*. 42 (2009) 1788.
3. M.K. Nazeerudin, A. Kay, I Rodicio, R. Huxnpbry-Baker E. Miiller, P. Liska. *J Am Chem Soc.* 115 (1993) 6382.
4. J. Sheng, L.H. Hu, S.Y. Xu, W.Q. Liu, L. Mo, H.J. Tian, S.Y. Dai, *Journal of Materials Chemistry* 21 (2011) 5457.
5. X.P. Lin, D.M. Song, X.Q. Gu, Y.L. Zhao, Y.H. Qiang, *Applied Surface Science* 263 (2012) 816.
6. D.M. Song, Y.H. Qiang, Y.L. Zhao, X.Q. Gu, C.B. Song, *Applied Surface Science* 277 (2013) 53.
7. M. Grätzel, *J. Photochem. Photobiol*. C 4 (2003) 145.
8. J.H. Yum, C. Peter, M. Grätzel, Md.K. Nazeeruddin, *ChemSusChem* 1 (2008) 699.
9. T.G. Deepak, G.S. Anjusree, S. Thomas, T.A. Arun, S.V. Nair, A.S. Nair, *RSC Advances* 4 (2014) 17615.
10. J.F. Yan, F. Zhou, *Journal of Materials Chemistry* 21 (2011) 9406.
11. H. Wang, Z.G. Guo, S.M. Wang, W.M. Liu, *Thin Solid Films* 558 (2014) 1.
12. H.M.A. Javed, W.X. Que, Z.L. He, *Journal of Nanoscience and Nanotechnology* 14 (2014) 1085.
13. X. Fang, M. Li, K. Gou, Y.Zhu, Z.Hu. *Electrochimica Acta* 65 (2012) 174.
14. E.S. Kwak, W. Lee, N.G. Park, J. Kim, H. Lee, *Adv. Funct.Mater*. 19 (2009) 1093.
15. T. Chen, G.H. Guai, C. Gong, W.H. Hu, J.X. Zhu, H.B. Yang, Q.Y. Yan, C.M. Li, *Energy Environ. Sci.* 5 (2012) 6294.
16. F.Z. Huang, D.H. Chen, X.L. Zhang, R.A. Caruso, Y.B. Cheng, *Adv. Funct. Mater*. 20 (2010) 1301.
17. K.S. KNovoselov, A.K. Geim, S.V. Morozov, D. Jiang, M.I. Katsnelson, I.V. Grigorieva, et al. *Nature* 438 (2005) 197.
18. A.H. Castro Neto, F. Guinea, N.M.R. Peres, K.S. Novoselov, A.K. Geim. *Rev Mod Phys* 81 (2009) 109.
19. L.X. Dong, Q. Chen, *Front. Mater. Sci. China* 4 (2010) 45.
20. M. Song, H.K. Seo, S. Ameen, M.S. Akhtar, H.S. Shin, *Electrochimica Acta* 115 (2014) 559.
21. F. Bonaccorso, Z. Sun, T. Hasan, A.C. Ferrari. *Nat Photonics* 4 (2010) 611.
22. M.D. Stoller, S.J. Park, Y.W. Zhu, J.H. An, R.S. Ruoff. *Nano Lett*. 8 (2008) 3498.
23. P. Wang, J. Wang, T.S. Ming, X.F. Wang, H.G. Yu, J.G. Yu, Y.G. Wang, M. Lei, *Applied Materials & Interfaces* 5 (2013) 2924.
24. A. Geim, K. Novoselov, *Science* 324 (2009) 875.
25. D.W. Zhang, X.D. Li, H.B. Li, S. Chen, Z. Sun, X.J. Yin, S.M. Huang. *Carbon*. 49 (2011) 5382.
26. A-Young Kim, Jieun Kim, *Bull. Korean Chem. Soc*. 33 (2012) 10.
27. X.L. Fang, M.Y. Li, K.M. Guo, Y.D. Zhu, Z.Q. Hu, X.L. Liu, B.L. Chen, X.Z. Zhao, *Electrochimica Acta* 65 (2012) 174.
28. L. Chen, Y. Zhou, W.G. Tu, Z.D. Li, C.X. Bao, H. Dai, T. Yu, J.G. Liu, Z.G. Zou, *Nanoscale* 5 (2013) 3481.
29. T. Chen, W.H. Hu, J.L. Song, G.H. Guai, C.M. Li. *Adv. Funct. Mater*. 22 (2012) 5245.
30. S.R. Sun, L. Gao, Y.Q. Liu, *Appl. Phys. Lett*. 96 (2010).
31. N.L. Yang, J. Zhai, D. Wang, Y.S. Chen, L. Jiang, *ACS Nano* 4 (2010) 887.
32. Y.B. Tang, C.S. Lee, J. Xu, Z.T. Liu, Z.H. Chen, Z.B. He, Y.L. Cao, G.D. Yuan, H.S. Song, L.M. Chen, L.B. Luo, H.M. Cheng, W.J. Zhang, I. Bello, S.T. Lee, *ACS Nano* 4 (2010) 3482.

33. H. Wang, Y.H. Hu, *Ind. Eng. Chem. Res*. 50 (2011) 6132.
34. W.S. Hummers, R.E. Offema, *J. Am. Chem. Soc*. 80 (1958) 1339.
35. M. R. Golobostanfard, H. Abdizadeh, *Sol. Energy Mater. Sol. Cells* 120 (2014) 295.
36. P. F. Du, L. X. Song, J. Xiong, N. Li, L. J.Wang, Z. Q. Xi, N. Y. Wang, L. H. Gao, H. L. Zhu, *Electrochim. Acta* 87 (2013) 651.
37. B. Tang, G. X. Hu, *J. Power Sources* 220 (2012) 95.
38. C.B. Song, Y.H. Qiang, Y.L. Zhao, X.Q. Gu, D.M. Song, L. Zhu, *Applied Surface Science* 305 (2014) 792.
39. Y.L. Zhao, D.M. Song, Y.H. Qiang, X.Q. Gu, L. Zhu, C.B. Song, *Applied Surface Science* 309 (2014) 85.
40. L. Zhu, Y.L. Zhao, X.P. Lin, X.Q. Gu, Y.H. Qiang, *Applied Surface Science* 65 (2014) 152.
41. T.W. Hamann, R.A. Jensen, A.B.F. Martinson, H.V. Ryswyk, J.T. Hupp, *Energy Environ. Sci*. 1 (2008) 66.